Advances in Robotics & Automation
ISSN: 2168-9695

Rahman et al., Adv Robot Autom 2017, 6:3
DOI: 10.4172/2168-9695.1000178

Research Article Open Access

Study on Tracked Combine Harvester Dynamic Model for Automated Navigation Purposes

Rahman M M[1], Ishii K[2]* and Noguchi N[2]

[1]*Graduate School of Agriculture, Hokkaido University, Kita-9, Nishi-9, Kita-ku, Sapporo 060-8589, Japan*
[2]*Research Faculty of Agriculture, Hokkaido University, Kita-9, Nishi-9, Kita-ku, Sapporo 060-8589, Japan*

Abstract

This research describes the tracked combine harvester dynamic model developed based on the sensor measurements for the controlling of tracked combine harvester and the application of automated navigation. Real time global positioning system and inertial measurement unit were equipped on the tracked combine harvester for obtaining the position, direction of travel, angular rate etc. Circular and sinusoidal trajectories were performed by the tracked combine harvester over the concrete and soil ground from a set of steering commands to evaluate the tracked combine harvester dynamic model. The results indicate that the computed harvester state, angular yaw rate, soil parameter, track coefficients, turning radius and sideslip angle from the tracked combine harvester dynamic model and sensor measurements can be used to control an autonomous tracked combine harvester during non-linear maneuverability.

Keywords: Tracked combine harvester; RTK-GPS; IMU; Dynamic model

Introduction

Tracked vehicles are widely popular in off-road mobile robot applications such as military and agricultural industries due to their mechanical configuration, maneuverability and traction. The controlling mechanisms of tracked vehicle are quite different than wheeled vehicles because of non-linear characteristics between the track and the ground. Mathematical modeling of tracked vehicles is required in determining the vehicle state, heading of vehicle, compensation of sensor uncertainties for controlling of an autonomous off-road tracked vehicle. Literatures related to a tracked vehicle are described a kinematic and dynamic models, which have been developed to account track-soil interaction parameters at different terrain condition [1,2]. Tracked vehicle state estimation, direction of vehicle, soil parameter and track coefficients based on the concept of kinematic and dynamic models are essential to achieve precise, robust autonomous guidance and control of a tracked vehicle in real time.

Soil parameter and track coefficients play an important role in determining the maximum track forces and moment of turning resistance developed by the tracked vehicles, which is a little bit difficult to measure in real time. A few researches have been done to estimate the soil parameter and track coefficients by using the theoretical and statistical methods. For instance, a method is described for estimating slip with a statistical method from the vehicle trajectory data, and sideslip angle for a tracked vehicle in real time [3,4]. A methodology for calculating track coefficient is described for small to large scaled tracked vehicle for a terrain [2,5]. The estimation of track coefficient is also obtained with statistical method using the kinematic and dynamic model for a different terrain [6], and this result confirmed the dependence of track coefficient on vehicle turning radius and velocity [7]. In addition, the turning radius is a vital parameter for turning maneuverability that is estimated theoretically from the vehicle speed and angular rate based on kinematic model [1,2]. But, these above parameters can be obtained in this research from the vehicle controlling parameters, position and inertial sensor measurements combined with the tracked kinematic and dynamic model.

In autonomous navigation of tracked combine harvester, the state and posture can be obtained from the positioning and inertial sensor measurements. But these sensor measurements have measurement uncertainties, which can be compensated by using the tracked combine harvester kinematic and dynamic model. On the other hand, the computation of soil parameter and track coefficients are also important for the tracked combine harvester dynamic model. An autonomous tracked combine harvester is developed in the vehicle robotics laboratory, Hokkaido University based on Real Time Kinematic Global Positioning System (RTK-GPS) and Inertial Measurement Unit (IMU) for the harvesting of wheat and paddy [8]. Due to consider non-linear characteristics between the tracked combine harvester and terrain, and sensor measurement uncertainties, tracked combine harvester dynamic model is required for controlling precisely. For considering this matter, a tracked combine harvester dynamic model is developed based on Wong [2] with relevant sensor measurements in this research. Consequently, these tracked model equations are also used to determine the soil parameter and track coefficients of tracked combine harvester. In addition, the turning radius is obtained from the tracked combine harvester position by using the regression model, which is a good approach than theoretical turning radius. Therefore, the overall objectives concentrate in this research to develop a tracked dynamic model integrated with the positioning and inertial sensor measurements, which can be further used for the controlling of autonomous tracked combine harvester in non-linear condition, and also for the navigation application.

***Corresponding author:** Kazunobu Ishii, Research Faculty of Agriculture, Hokkaido University, Japan, Tel: +81-11-706-3626; E-mail: ici@bpe.agr.hokudai.ac.jp

Received November 20, 2017, **Accepted** November 27, 2017, **Published** December 01, 2017

Citation: Rahman M M, Ishii K, Noguchi N (2017) Study on Tracked Combine Harvester Dynamic Model for Automated Navigation Purposes. Adv Robot Autom 6: 178. doi: 10.4172/2168-9695.1000178

Citation: Rahman M M, Ishii K, Noguchi N (2017) Study on Tracked Combine Harvester Dynamic Model for Automated Navigation Purposes. Adv Robot Autom 6: 178. doi: 10.4172/2168-9695.1000178

Materials and Methods

System components

This research was conducted on a YANMAR AG1100 Tracked Combine Harvester which is equipped with an on- board computer to log sensor measurements from the RTK-GPS and IMU sensors by using serial ports as shown in Figure 1. This tracked combine harvester is fully controlled by a Control Area Networking (CAN bus). The speed limit for the tracked combine harvester is maintained up to 2 m/s, and it is used for harvesting cereal crops such as paddy, wheat and even soybean.

The RTK-GPS was used to measure position, direction of travel and speed of the tracked combine harvester. 5-10 Hz update rate and 115200 Baud rate were used to fix for the RTK mode, where the maximum update and output rates of RTK-GPS is up to 20 Hz. The RTK correction signal was calculated from a Virtual Reference System (VRS) via an Internet connected to the on-board computer that logs the data from the GPS receiver through RS232C serial port. The IMU (VECTORNAV, VN-100) sensor was used as posture sensor, which measures the angular rate of the tracked combine harvester. The output signals from the IMU were logged at a frequency of 200 Hz through a RS232C serial port.

Figure 1: Outlook of the tracked combine harvester equipped with RTK-GPS and IMU sensors.

Tracked combine harvester dynamic model

Figure 2 shows the free body diagram of dynamic model for the tracked combine harvester which is moving on a general plane [1,2,4,6], turning to the left or counter clockwise, where its acceleration is in the positive x,y and φ directions. The external thrusts and resistive forces acting on the tracked combine harvester are F_R, F_L and R_R, R_l, respectively. The value f_y indicates the lateral friction force due to the effect of lateral soil shear.

The Figure 2a is shown in the global reference frame XYZ; which indicates the tracked combine harvester turns around an instantaneous center of rotation (ICR). The angle β is called side slip angle, which is determined from the velocity V_c and the longitudinal axis x of the tracked combine harvester. It is assumed that the normal pressure distribution along the track is non-uniform, and the coefficient of lateral resistance μ is not constant. The instantaneous center of rotation must shift forwards of the tracked combine harvester centroid by the amount of D, as shown in Figure 2a, and this longitudinal shifting D depends on the tracked combine harvester lateral acceleration [2]. D is required to develop a net lateral force that accelerates the tracked combine harvester towards the instantaneous center of rotation, and also minimizes the resistive yawing moment [3]. Using RTK-GPS and IMU sensor measurements along with the tracked combine harvester internal parameters, the dynamic motion model equation can be modified in order to calculate some essential parameters for automated navigation purposes. For a tracked combine harvester of mass m and a moment of inertia about the center of mass I, the equations of dynamic motion can be written in the body reference frame by using eqns. (1-3), respectively.

$$m\ddot{x}_c = F_R + F_L - R_R - R_L - F_c\sin\beta \tag{1}$$

$$m\ddot{y}_c = F_c\cos\beta - \mu mg \tag{2}$$

$$I\ddot{\varphi} = \frac{\left[\left(F_R - R_R\right) - \left(F_L - R_L\right)\right]B}{2} - M_r \tag{3}$$

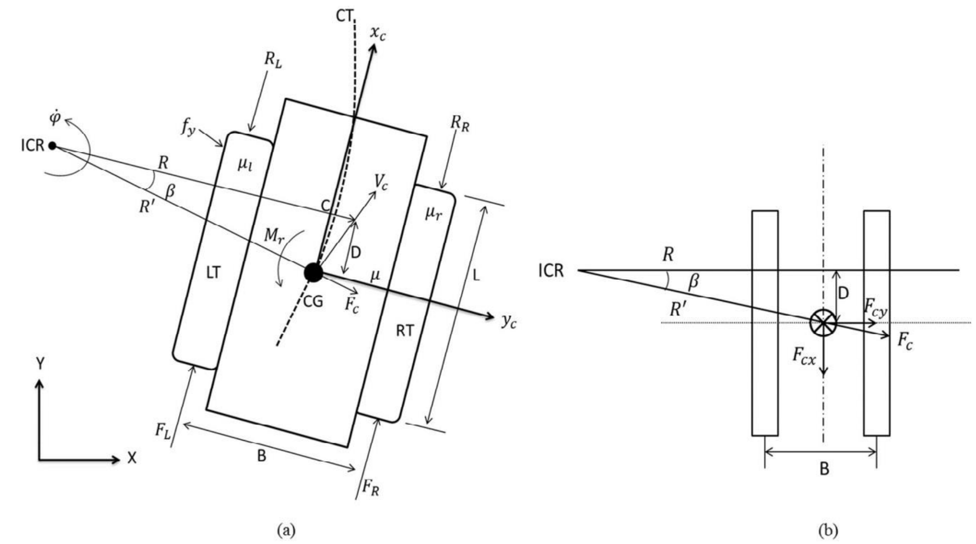

Figure 2: Free body diagram of the tracked combine harvester dynamic model (a. General forces acting on the harvester and b. Detail of centrifugal force, F_c).

Where, the suffix c denotes coordinates fixed on the combine harvester. The centrifugal force F_C acting on the tracked combine harvester is shown in Figure 2b. The resultant F_C is given by $F_c = \frac{mV_c^2}{R}$; and the longitudinal and lateral centrifugal forces are given by eqns. (4) and (5), respectively.

$$F_{cx}\sin\beta = \frac{mV_c^2}{R}\sin\beta \quad (4)$$

$$F_{cy}\cos\beta = \frac{mV_c^2}{R}\cos\beta \quad (5)$$

The sideslip angle β is calculated from the difference between the direction of the tracked combine harvester given by the RTK-GPS and the heading given by the IMU [9].

$$\beta = \varphi_{gps} - \varphi_{imu} \quad (6)$$

The thrust forces on right and left tracks are determined by eqns. (7) and (8); where, μ_r and μ_l indicates the longitudinal coefficient of friction for the right and left tracks and B is the distance between two tracks.

$$F_R = \frac{mg\left(2B\mu_r + \mu L\right)}{4B} \quad (7)$$

$$F_L = \frac{mg\left(2B\mu_l - \mu L\right)}{4B} \quad (8)$$

It is considered that the centrifugal forces also cause lateral load transfer. That why, the longitudinal resistive forces of the right and left tracks will not be identical, as described by eqns. (9) and (10). Where, H, $\dot{\varphi}$, and R are the height of center of gravity, angular rate and turning radius of the tracked combine harvester.

$$R_R = \left(\frac{mg}{2} + \frac{Hm\dot{\varphi}^2 R}{B}\right)\mu_r \quad (9)$$

$$R_L = \left(\frac{mg}{2} - \frac{Hm\dot{\varphi}^2 R}{B}\right)\mu_l \quad (10)$$

The moment of turning resistance M_r around the centers of the tracks for the tracked combine harvester is given by eqn. (11).

$$M_r = \frac{\mu mgL}{4} \quad (11)$$

Where, the lateral coefficient of friction μ depends on the turning radius R, angular rate φ, and side slip angle β of the tracked combine harvester which is calculated by using eqn. (12).

$$\mu = \frac{1}{g}\left(\dot{\varphi}^2 R - \frac{\Delta V_c}{\Delta t} tan\beta\right) \quad (12)$$

Using the lateral coefficient of friction μ, the longitudinal coefficient of friction for the right and left tracks are calculated by using eqns. (13) and (14), where V_R and V_L are the right and left tracks velocities of the tracked combine harvester.

$$\mu_r = \frac{2}{g}\left[\frac{\Delta V_R}{\Delta t} - \frac{gL}{4B}\mu\right] \quad (13)$$

$$\mu_l = \frac{2}{g}\left[\frac{\Delta V_L}{\Delta t} + \frac{gL}{4B}\mu\right] \quad (14)$$

Tracked combine harvester kinematic model

Figure 3 shows the tracked combine harvester turning around an instantaneous center of rotation (ICR). Consider, the velocities of right and left tracks are V_R and V_L; with the slip velocities V_{sr} and V_{sl}, the turning radius R and angular rate $\dot{\varphi}$ are expressed by eqn. (15) [1].

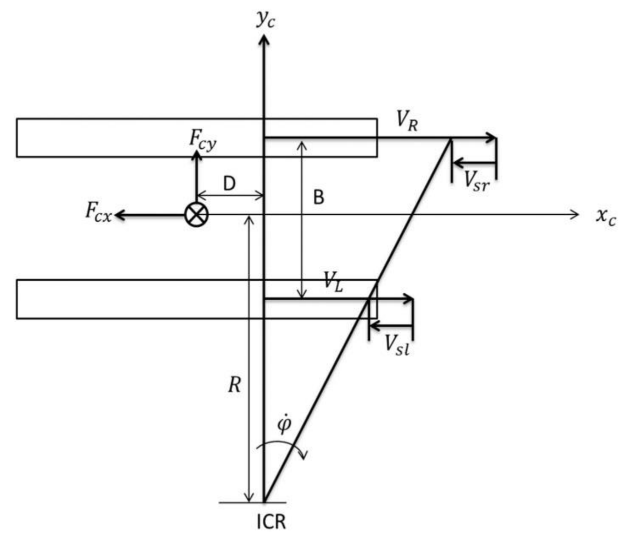

Figure 3: Schematic diagram of the tracked combine harvester's speed, slip velocity and turning radius.

$$R\dot{\varphi} = \frac{1}{2}[V_R - V_{sr} + V_L - V_{sl}] \quad (15)$$

Using the eqn. (15), the theoretical radius R is obtained by the eqn. (16).

$$R = \frac{\left[V_R\left(1 - S_r\right) + V_L\left(1 - S_l\right)\right]}{2\dot{\varphi}} \quad (16)$$

Where, the slip of left and right tracks is computed by the following eqns. (17) and (18), respectively.

$$S_l = 1 - \frac{2V_{gps} - B\dot{\varphi}}{2V_L} \quad (17)$$

$$S_r = 1 - \frac{2V_{gps} + B\dot{\varphi}}{2V_R} \quad (18)$$

The vehicle's velocity V_C is calculated based on the each track velocity including the slip of track from the tracked combine harvester expressed by the eqn. (19).

$$V_c = \frac{V_R\left(1 - S_r\right) + V_L\left(1 - S_l\right)}{2} \quad (19)$$

Figure 4 shows the RTK-GPS position which is used to calculate the actual turning radius R by using the least square method, whilst the general circle equation is indicated by the eqn. (20).

$$(a-x)^2+(y-b)^2=R^2 \quad (20)$$

With the least squares, "best fit" means the equation have to minimize which is

$F(h, k, R) = \sum[(x_i - h)^2 + (y_i - k)^2 - R^2]^2$. Now, the circle equation can be linearized by the eqn. (21).

$$x^2+y^2=Ax+By+C \quad (21)$$

Where, A, B and C are undetermined coefficients in eqn. (21). To

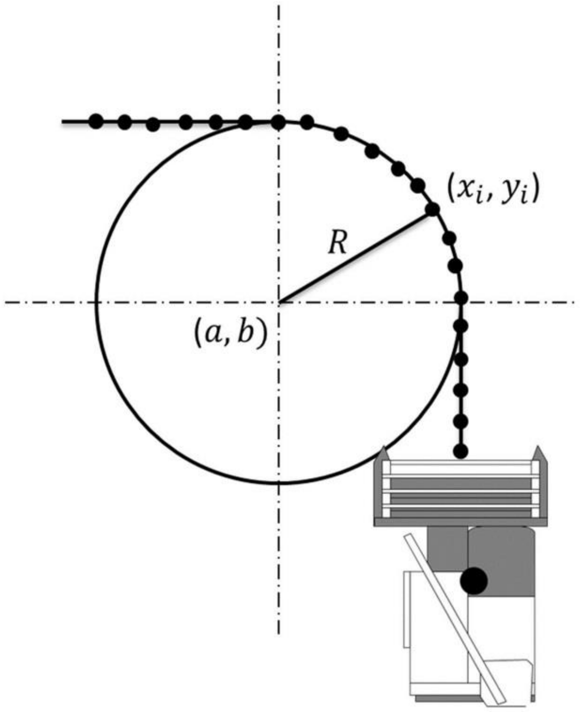

Figure 4: Turning radius *R* calculated from the GPS position.

compute these coefficients, a matrix equation developed for circular regression is arranged as shown in the eqn. (22).

$$\begin{bmatrix} \sum x_i^2 & \sum x_i y_i & \sum x_i \\ \sum x_i y_i & \sum y_i^2 & \sum y_i \\ \sum x_i & \sum y_i & n \end{bmatrix} \begin{bmatrix} A \\ B \\ C \end{bmatrix} = \begin{bmatrix} -\sum\left(x_i^3 + x_i y_i^2\right) \\ -\sum\left(x_i^2 y_i + y_i^3\right) \\ -\sum\left(x_i^2 + y_i^2\right) \end{bmatrix} \tag{22}$$

Where n is the number of RTK-GPS positions (x_i, y_i). In eqn. (22), if the left side matrix is invertible, the values of *A, B* and *C* generate the circle of best fit. After obtaining *A, B* and *C*, the center of the circle and the turning radius *R* are obtained by using eqns. (23) and (24).

$$a = -\frac{A}{2}, b = -\frac{B}{2} \tag{23}$$

$$R = \sqrt{(a^2 + b^2 - C)} \tag{24}$$

By computing turning radius *R*, it is necessary to fix the direction (left and right turn) of the tracked combine harvester. For the direction of turning radius *R*, the eqn. (25) is used and made a condition based on cross product using the circle center and RTK-GPS positions (where, *i=0,1,2…*).

$$(a_i - x_i)(y_{i+1} - y_i) - (b_i - y_i)(x_{i+1} - x_i) \begin{cases} > 0; R > 0 \text{ for right turn} \\ < 0; R < 0 \text{ for left turn} \end{cases} \tag{25}$$

Now, the eqns. (1) and (2) are integrated to make the velocities of longitudinal and lateral direction for the tracked combine harvester in local coordinate. In order to operate the tracked combine harvester in real time, the velocities of longitudinal and lateral direction in the harvester coordinate is expressed as a global reference frame by the eqn. (26).

$$\begin{bmatrix} \dot{X} \\ \dot{Y} \end{bmatrix} = \begin{bmatrix} cos\varphi & -sin\varphi \\ sin\varphi & cos\varphi \end{bmatrix} \begin{bmatrix} \dot{x}_c \\ \dot{y}_c \end{bmatrix}. \tag{26}$$

Methods

This dynamic system was verified by the field experiment in the Hokkaido University agricultural field. The tracked combine harvester with a proper configuration of RTK-GPS and IMU sensors were used during the experiment. In this case, the tracked combine harvester was moved on the concrete and soil ground. A set of input steering angles were fixed to run the tracked combine harvester at a circular and a sinusoidal trajectories. A constant 30 deg. of steering angle was chosen for circular trajectory; whereas ± 30 deg. steering command was for sinusoidal trajectory. Completely running at circular and sinusoidal trajectories, the position, direction and speed of the tracked combine harvester from RTK-GPS and angular rate from IMU were used to obtain the state of the harvester, track-soil interaction parameter, and track coefficients by using the tracked combine harvester motion model. The turning radius *R* was calculated based on the RTK-GPS positions by the eqn. (24) for tuning maneuverability. C/C++ programing language was used to describe the above parameters in this research.

Results and Discussion

Figure 5 shows the circular and sinusoidal trajectories of the tracked combine harvester on a concrete and soil ground in the agricultural field side of Hokkaido University, Japan, which was obtained from the measured and dynamic model. The measured trajectory is obtained from the fixed RTK-GPS on the tracked combine harvester with a set of input steering commands. Figure 5a and 5b indicates the circular trajectories on the concrete and soil ground while steering angle was 30°. The sinusoidal trajectories were obtained by a series of steering angle (± 30°) as shown in Figure 5c and 5d. The results showed that the dynamic model trajectories of tracked combine harvester matched with the measured trajectories fairly well. From the error analysis of circular trajectories, the RMS errors between the measured and dynamic model for the concrete and soil ground are 0.029 m and 0.012 m, respectively. The RMS error for concrete ground is higher than soil one because of sliding the tracked combine harvester on concrete ground. The RMS errors of sinusoidal trajectories are 0.034 m for concrete ground and 0.032 m for soil ground. This result indicates that the dynamic model trajectories for both grounds are consistent to the measured one.

Figure 6 shows the measured and dynamic model yaw rate $\dot{\varphi}$ of the tracked combine harvester for the circular and sinusoidal trajectories. The measured yaw rate $\dot{\varphi}$ was obtained directly from the IMU sensor while the dynamic model yaw rate $\dot{\varphi}$ was calculated from the dynamic model equation. The dynamic model yaw rate $\dot{\varphi}$ can be influenced by the yaw moment of inertia *I* because it is a divisor factor. The yaw moment of inertia *I* is very important that reflects the tracked combine harvester's resistance to change its direction; which means a big yaw moment of inertia *I* makes the combine harvester slower to swerve or go into a tight curve, and it also makes it slower to turn straight again [10]. The RMS error of yaw rate $\dot{\varphi}$ obtained from the measured and dynamic model is 0.0004 rad/sec for both grounds of circular and sinusoidal trajectories. The RMS error indicates that the yaw rate $\dot{\varphi}$ given by the dynamic model is closest to the measured yaw rate $\dot{\varphi}$.

The speed of tracked combine harvester for circular and sinusoidal trajectories on a concrete and soil ground is shown in Figure 7. The results indicate that the speed is not constant all over the time; which varies time to time.

Figure 8 shows the theoretical sideslip angle β that was calculated from the equation $\beta = tan^{-1}\left(\frac{\dot{X}}{\dot{Y}}\right)$ and compared with the measured

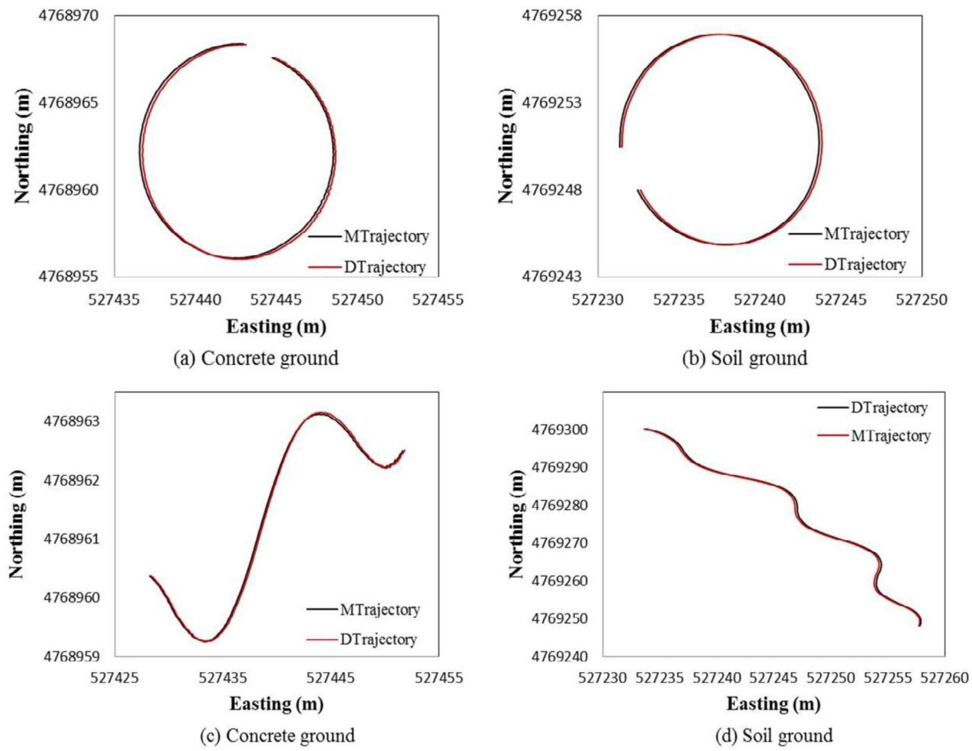

Figure 5: Measured Trajectory (MTrajectory) and Dynamic model trajectory (DTrajectory) of the tracked combine harvester which runs in a circular and sinusoidal way.

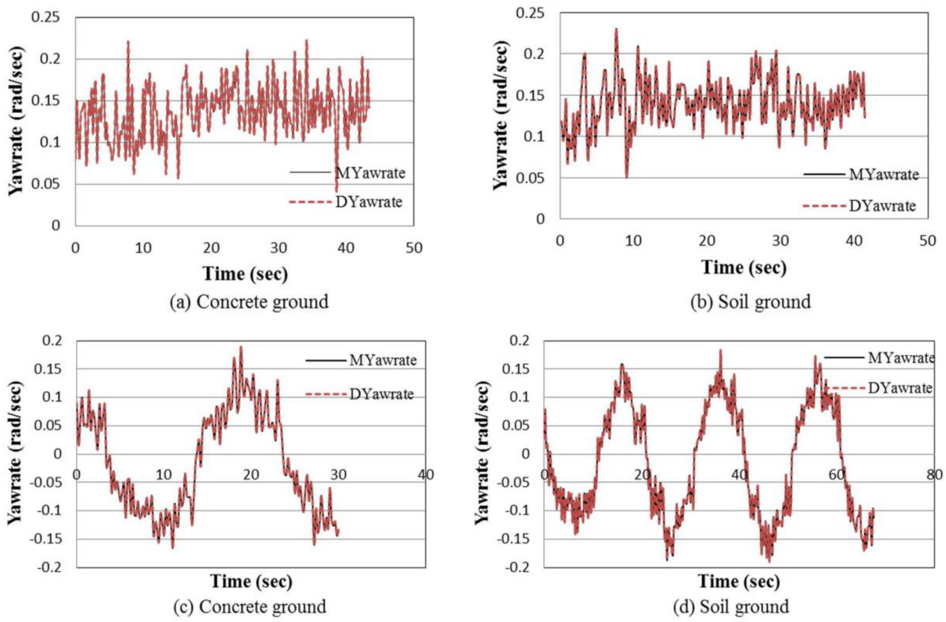

Figure 6: Measured yaw rate (MYawrate) and Dynamic model yaw rate (DYawrate) of the tracked combine harvester which runs in a circular and sinusoidal way.

sideslip angle β obtained from the heading difference of RTK-GPS and IMU. For the circular and sinusoidal trajectories of tracked combine harvester for the soil ground, the RMS error between the measured and theoretical sideslip angle β is about 2.5°; which means the measured and theoretical sideslip angle are consistent. But the RMS error of sideslip angle β over concrete ground for the circular and sinusoidal trajectories is about 4.0°. because of sliding the tracked combine harvester on the concrete surface. In addition, the fluctuation of sideslip angle β is caused by the integration of yaw rate, noisy GPS direction angle and speed of the tracked combine harvester. A low speed with

Citation: Rahman M M, Ishii K, Noguchi N (2017) Study on Tracked Combine Harvester Dynamic Model for Automated Navigation Purposes. Adv Robot Autom 6: 178. doi: 10.4172/2168-9695.1000178

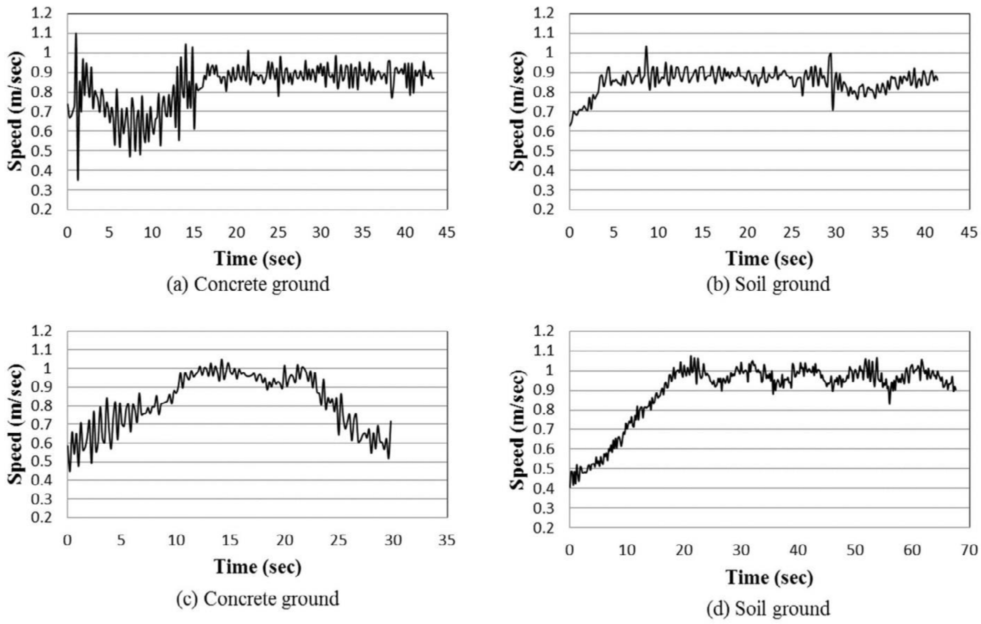

Figure 7: Speed of tracked combine harvester for circular and sinusoidal trajectories.

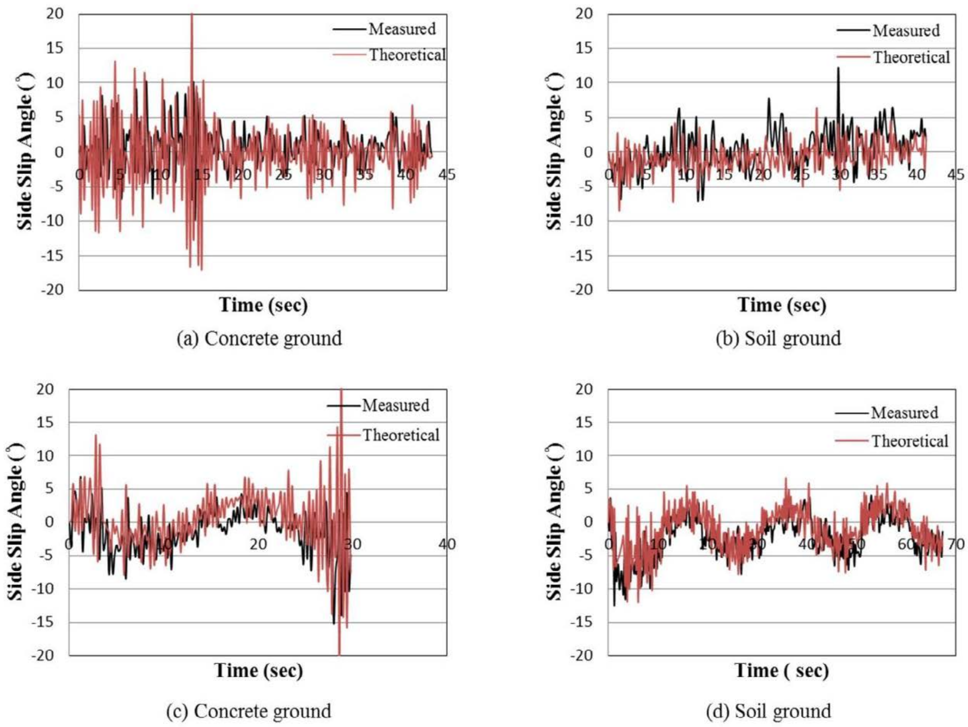

Figure 8: Measured and theoretical sideslip angle β for the circular and sinusoidal trajectories.

a high steering angle can make a little bit large sideslip angles [11]. In addition, the speed of the tracked combine harvester is not uniform that influences the change of the direction of tracked combine harvester suddenly and makes a large fluctuation of sideslip angle β.

Figure 9 shows a theoretical and measured turning radius R over time for circular and sinusoidal trajectories calculated by eqns. (16) and (24). The measured turning radius R was calculated from the RTK-GPS position of tracked combine harvester. The smoothness of measured turning radius R depends on the number of RTK-GPS points chosen for the regression analysis by using the eqn. (24). The turning radius R for circular trajectories is almost constant with small fluctuation. The average turning radius R for circular trajectories is 6.0 m as shown in Figure 9a and 9b. On the other hand, theoretical turning radius R was estimated for the evaluation of our measured turning radius. Unlike

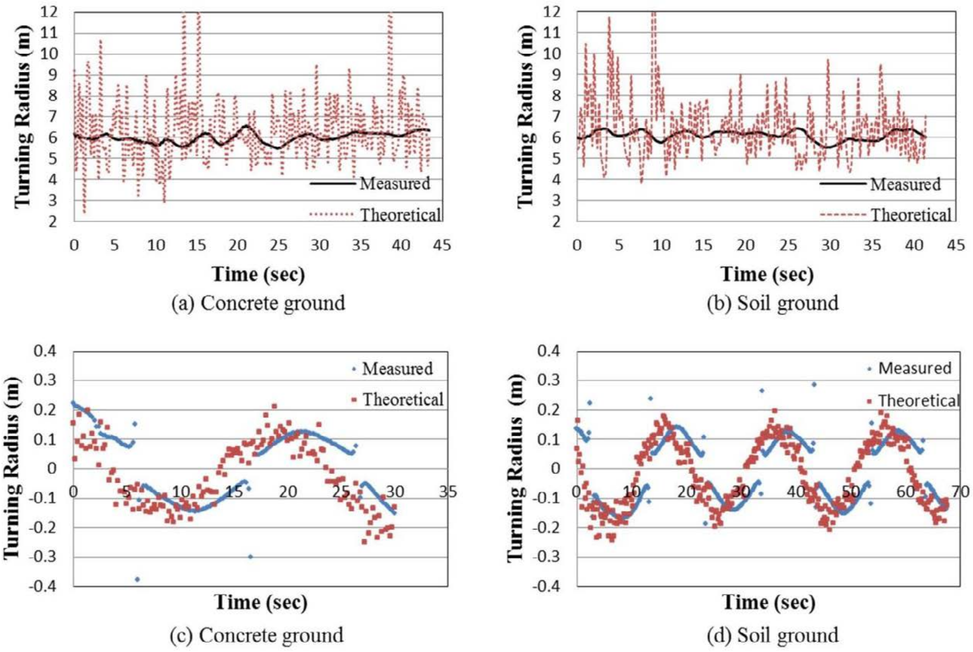

Figure 9: Measured and theoretical turning radius R for circular and sinusoidal trajectories.

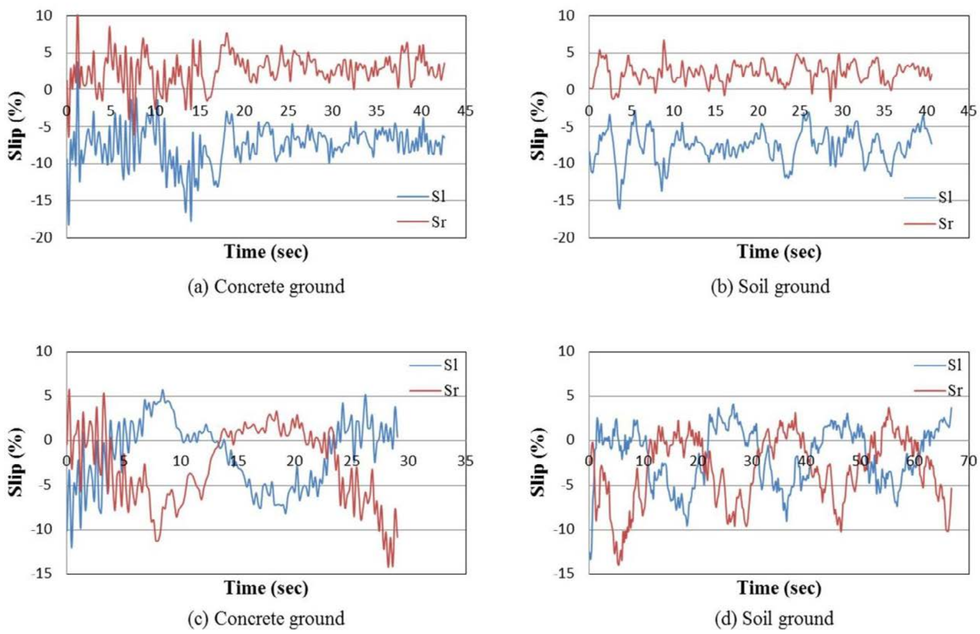

Figure 10: Computed slip of left and right tracks for the circular and sinusoidal trajectories.

measured turning radius, theoretical turning radius is noisy but shows the similar trend. Theoretical output is influenced by the yaw rate and speed of the tracked combine harvester. Figure 9c and 9d shows the inverse turning radius *R* for sinusoidal trajectories over time for concrete and soil ground. The inverse turning radius describes the continuous motion of the tracked combine harvester. The results reveal that the harvester turns to the left side, the turning radius *R* will be negative; otherwise turning radius *R* will be positive for a right turn. Theoretical turning radius *R* is noisy but it's give a similar sinusoidal shape as measured turning radius.

Figure 10 shows the slip S_l and S_r for left and right tracks for circular and sinusoidal trajectories that was estimated by eqns. (17) and (18), respectively. The slip of circular and sinusoidal trajectories for concrete and soil ground is almost same, but this result may be influenced by the steering command. When the tracked combine harvester runs both circular and sinusoidal trajectories, the slip will increases significantly with the increasing of steering command in order to generate the track thrusts which can be used to overcome the turning moment resistance. This track thrusts may introduce a high slip of the outer track.

Citation: Rahman M M, Ishii K, Noguchi N (2017) Study on Tracked Combine Harvester Dynamic Model for Automated Navigation Purposes. Adv Robot Autom 6: 178. doi: 10.4172/2168-9695.1000178

By using the eqn. (12), the lateral coefficient of friction μ was computed for the circular and sinusoidal trajectories. Figure 11 shows the lateral coefficient of friction μ on concrete and soil ground for the tracked combine harvester over time. The lateral coefficient of friction μ may be varied with the high thrust and small turning radius as compared to large turning radius [12]. The results reveal that the estimated lateral coefficient of friction μ for both concrete and soil ground are same due to same turning radius R, but it may be higher for large steering command as compared to the small steering command.

Figure 12 shows the longitudinal coefficient of friction μ_l and μ_r for the left and right tracks for circular and sinusoidal trajectories on concrete and soil grounds. The longitudinal coefficient of friction depends on the steering command, turning radius and lateral coefficient of friction; which may be changed from terrain to terrain. The longitudinal coefficient of friction μ_l and μ_r for the left and right tracks by using eqns. (13) and (14) are almost same for both grounds, but it can increase when the steering angle increases or turning radius decreases as shown in Figure 12.

Conclusions

This paper describes the tracked combine harvester dynamic model integrated with the positioning and inertial sensor measurements to control the tracked combine harvester in non-linear characteristics. Based on the dynamic model and sensor measurements, the soil

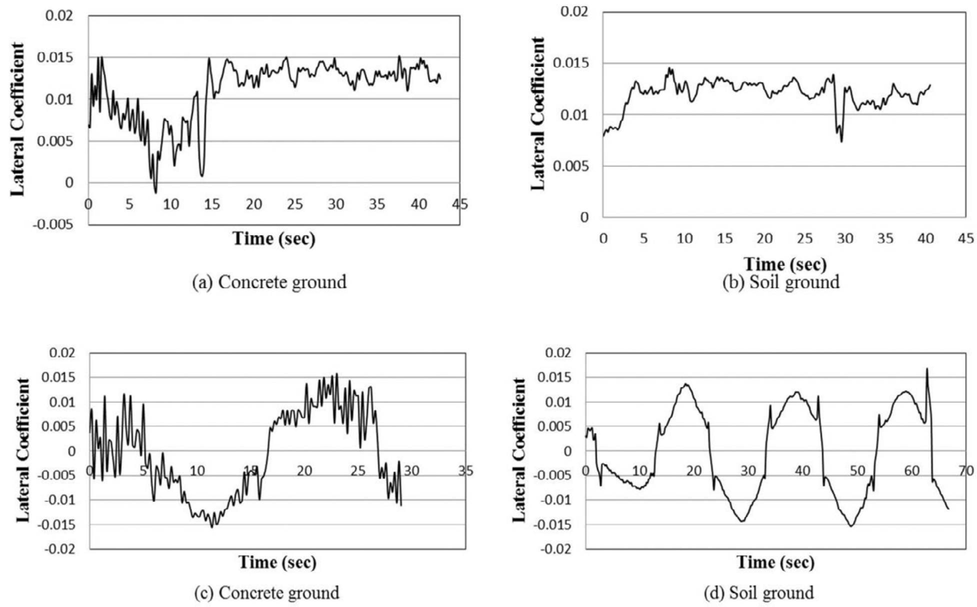

Figure 11: Lateral coefficient of circular and sinusoidal trajectories for concrete and soil ground.

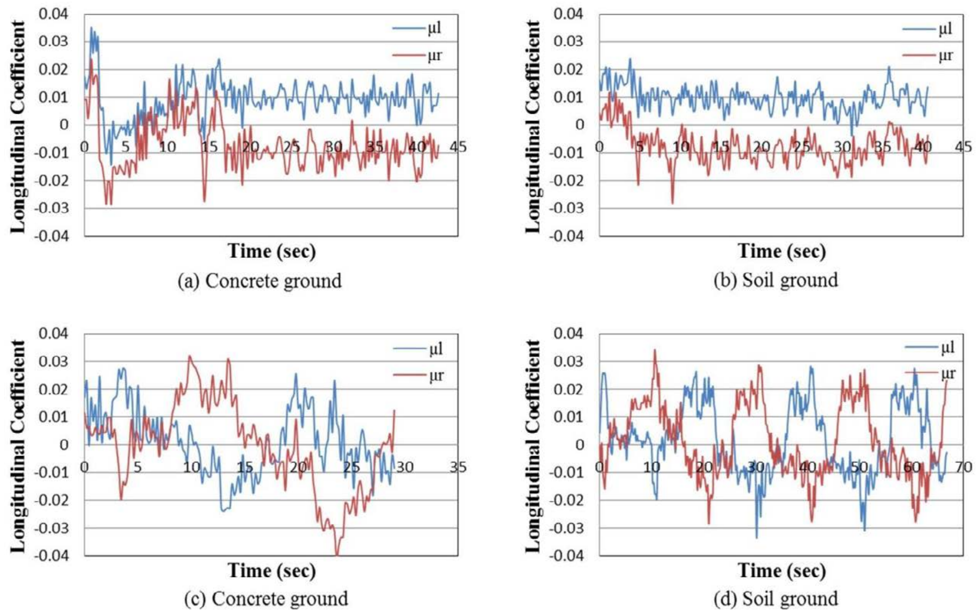

Figure 12: Longitudinal coefficient of friction for the left and right tracks computed for circular and sinusoidal trajectories on the concrete and soil ground.

interaction parameter and track coefficients are obtained. The results of computed slip and track coefficients can be changed in terrain to terrain due to change of the tracked combine harvester steering and turning radius. The tracked combine harvester dynamic model is also verified by estimating the harvester state based on the sensor measurements. The turning radius from the RTK-GPS positions using regression model is better than theoretical turning radius. In addition, based on the computed track slip, sideslip angle, track coefficients and turning radius, the dynamic model can be used to control the autonomous tracked combine harvester precisely for non-linear condition in all terrain. In future research, the uncertainties of sensor measurements will be compensated by using this tracked combine harvester model specifically during turning maneuverability.

References

1. Kitano M, Jyozaki H (1976) A theoretical analysis of steerability of tracked vehicles. Journal of Terramechanics 13: 241-258.
2. Wong JY (2008) Theory of ground vehicles. A Wiley-Interscience Publication, New York, p: 592.
3. Le AT, Rye DC, Durrant-Whyte HF (1997) Estimation of track-soil interactions for autonomous tracked vehicles. Proceedings of International conference on robotics and automation.
4. Tehmoor MD, Raul GL (2010) Slip estimation for small-scale robotic tracked vehicles. Proceedings of the 2010 American control conference.
5. Kitano M, Kuma M (1977) An analysis of horizontal plane motion of tracked vehicles. Journal of Terramechanics 14: 211-225.
6. Tehmoor MD, Raul GL (2010) Estimating traction coefficients of friction for small-scale robotic tracked vehicles. Proceedings of the ASME dynamic systems and control conference, pp: 157-164.
7. Al-Milli S, Altheofer K, Seneviratne LD (2007) Dynamic analysis and traversability prediction of tracked vehicles on soft terrain. IEEE International conference on Networking, Sensing and Control.
8. Zhang Z, Noguchi N, Ishii K, Yang L, Zhang C, et al. (2013) Development of a Robot Combine Harvester for Wheat and Paddy Harvesting. IFAC Proceedings 46: 45-48.
9. Bevly DM (2004) Global Positioning System (GPS): A Low-Cost Velocity Sensor for Correcting Inertial Sensor Errors on Ground Vehicles. Journal of Dynamic Systems Measurement and Control 126: 255-264.
10. Ospina R, Noguchi N (2016) Determination of tire dynamic properties: Application to an agricultural vehicle. Engineering in Agriculture, Environment and Food 9: 123-130.
11. Bevly DM, Gerdes JC, Wilson C (2010) The use of GPS based velocity measurements for measurement of sideslip and wheel slip. Vehicle System Dynamics: International Journal of Vehicle Mechanics and Mobility 38: 127-147.
12. Wishmer RD, Luth HJ (1973) Off-road traction prediction for wheeled vehicles. Journal of Terramechanics 10: 49-61.